Asian Journal of Chemistry; Vol. 26, No. 12 (2014), 3569-3573

ASIAN JOURNAL OF CHEMISTRY

http://dx.doi.org/10.14233/ajchem.2014.16489

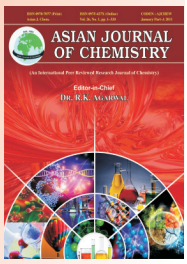

CdS-Sensitized TiO_2 Nanotube Arrays: Preparation and Enhanced Photocatalytic Activity

YUNSONG YUAN[1], LINGJIE LI[2], JINGLEI LEI[2,*], JIANXIN HE[2], JING XU[2] and SHENGTAO ZHANG[2]

[1]School of Urban Construction and Environmental Engineering, Chongqing University, Chongqing 400030, P.R. China
[2]School of Chemistry and Chemical Engineering, Chongqing University, Chongqing 400044, P.R. China

*Corresponding author: Fax: +86 23 65112328; Tel: +86 13983064116; E-mail: jllei@cqu.edu.cn

Received: 7 October 2013; *Accepted*: 28 February 2014; *Published online*: 5 June 2014; AJC-15296

CdS-sensitized TiO_2 nanotube arrays (CdS-TNTAs) were prepared by depositing CdS into the crystallized anodic TiO_2 nanotube arrays *via* sequential chemical bath deposition (S-CBD) method. Characterizations *via* XPS and FE-SEM show that the CdS nanoparticles, approximately 20-30 nm in diameter, were deposited on TiO_2 nanotubes arrays. UV-visible absorption spectra illustrate that sensitizing TiO_2 nanotubes with CdS extends the absorption response of TiO_2 nanotube arrays into the visible region. The photocatalytic efficiency of CdS-TNTAs is significantly enhanced as compared to the pristine TiO_2 nanotube arrays, which can be attributed to the deposition of CdS effectively stimulating the charge separation and thus hindering the recombination of electron/hole pairs of TiO_2 nanotube arrays. It is also demonstrated that the CdS deposition condition, such as the immersion time and cycles of sequential chemical bath deposition treatment, has important impacts on improving the photocatalytic efficiency of CdS-TNTAs. The appropriate immersion time (*e.g.* 5 or 10 min in the present work) and cycles (*e.g.* 2 or 1 cycle) of sequential chemical bath deposition process benefit the photocatalysis greatly.

Keywords: TiO_2 nanotube array, CdS, Anodization, Sequential chemical bath deposition, Photocatalysis, Methyl orange.

INTRODUCTION

As the most spectacular 1D TiO_2 nanostructure, TiO_2 nanotube arrays (TNTAs) that have large surface area and great adsorption capacity, exhibit high photocatalytic properties and photoelectric conversion efficiency[1-5]. They have a great potential in many applications, especially for photocatalysis[1-13]. Recently, TiO_2 nanotube arrays fabricated by the electrochemical anodization method have attracted special attention due to the facile fabrication process, fast charge transport properties and fabrication opportunity as well as a cost-effective scale-up process[1-5]. However, the inherent defects of TiO_2 materials, such as the wide band gap (3.1-3.2 eV), make TiO_2 nanotube arrays absorb only UV light, limiting the possibility of employing visible light that occupies the major part of solar light. Furthermore, the high rate of recombination of photogenerated electron/hole pairs often results in poor photocatalytic performance. To improve the photocatalytic efficiency, some methods have been developed, such as doping TiO_2 nanotube arrays with metal/nonmetal ions in order to induce red shift of the band gap[1-4,14-19] and coupling TiO_2 nanotube arrays with a low band gap semiconductor material, *e.g.*, CdS[1-4,20-23]. CdS is a relatively low band gap (2.4 eV) semiconductor which can be excited by visible light to produce photogenerated electrons and holes. Some scholars have reported that the photoactivity of TiO_2 nanotube arrays can be enhanced by sensitizing TiO_2 nanotubes with CdS[20-23], suggesting CdS-sensitized TiO_2 nanotube arrays (CdS-TNTAs) as promising systems for photocatalysis.

In the present work, CdS-TNTAs were prepared by depositing CdS into the crystallized anodic TiO_2 nanotubes *via* sequential chemical bath deposition (S-CBD) method[24], which is more facile and less cost-effective than the commonly used deposition methods of CdS, *e.g.*, electrochemical method[25,26], bifunctional linker coupling method[20,21]. The composition, morphology, UV-visible absorption features and photocatalytic activities in pollutant degradation of CdS-TNTAs are investigated. Specially, the effects of the immersion time and cycles of S-CBD treatment on the physical and chemical properties of CdS-TNTAs are studied.

EXPERIMENTAL

All chemicals (analytical grade; from Sinopharm Chemical Reagent Co., Ltd. Shanghai, PR China) were used as received, without further purification process. All solutions were prepared with deionized water.

Preparation of CdS-sensitized TiO_2 nanotube arrays: Titanium foils (99.4 % purity; 0.2 mm thickness) were obtained from Yunjie Metal Co., Ltd. (Baoji, P.R. China). Prior to anodization, the Ti foils were first mechanically polished with different abrasive papers and rinsed with deionized water. Then

they were chemically etched in a $HF/HNO_3/H_2O$ (1:5:4 in mass) mixture for 30 s and rinsed with deionized water. After that, they were ultrasonically degreased in acetone, isopropanol, methanol respectively for 5 min and finally rinsed with deionized water and dried in air. Anodization was performed at room temperature in a two-electrode bath, with the pretreated Ti foil as the working electrode and a platinum plate as the counter electrode. The anodization was conducted in 0.085M $H_2C_2O_4{\cdot}2H_2O$ + 0.5 wt. % NH_4F electrolyte at 20 V for 2 h. The voltage was applied using a DC power supply (DH1719A-5, Beijing Dahua Electronic Co., P.R. China). After anodization, the sample was rinsed with deionized water, dried in air and then annealed at 450 °C for 3 h to convert from the amorphous tubes to a defined anatase structure[12].

The CdS nanoparticles were deposited into the above crystallized TiO_2 nanotubes by sequential chemical bath deposition (S-CBD) method[24]. Typically, the sample was successively immersed in four different beakers for certain time in each beaker. One beaker contained 0.10 M $Cd(NO_3)_2$ aqueous solution, another contained 0.10 M Na_2S and the other two contained deionized water to rinse the samples from the excess of each precursor solution. Such an immersion cycle was repeated several times. Finally, the as-prepared samples were dried in air. To investigate the effects of the immersion time and cycles of S-CBD treatment (while keeping the whole S-CBD treatment duration as 40 min) on the physical and chemical properties of CdS-TNTAs, four types of samples were prepared. The corresponding S-CBD treatment conditions for the samples are listed in Table-1.

TABLE-1
CORRESPONDING S-CBD TREATMENT CONDITIONS FOR THE SAMPLES

Sample name	Immersion time in every solution during one cycle (min)	Cycle number	Whole S-CBD treatment duration (min)
$CdS_{0.5min/20C}$-TNTAs	0.5	20	40
$CdS_{1min/10C}$-TNTAs	1	10	40
$CdS_{5min/2C}$-TNTAs	5	2	40
$CdS_{10min/1C}$-TNTAs	10	1	40

FE-SEM, XPS and DRS characterization: The chemical composition of the sample was analyzed by X-ray photoelectron spectroscopy (XPS, Thermoelectron ESCALAB 250, USA) using MgK_α radiation as the X-ray source. The sample morphology was characterized using a field-emission scanning electron microscope (FESEM, FEI Nova 400, Holland). The cracked samples for cross-sectional observation were obtained by mechanically scraping. UV-visible absorption spectroscopy measurements were performed over the wavelength range of λ = 200-800 nm using a PUXI TU-1901 spectrophotometer (Beijing, PR China) equipped with a diffuse reflectance integration sphere attachment.

Photocatalytic activity measurements: The photocatalytic activities of the TiO_2 nanotubes samples were measured by the degradation test of an azo compound, methyl orange (MO). The photodegradation experiments were performed in a single-compartment photoreactor. The initial concentration of methyl orange was 10 mg/L. The photoirradiation was carried out with a 125-W blended fluorescent high pressure mercury lamp. Before the photocatalytic degradation, the samples were immerged into the target methyl orange solution for 0.5 h to establish the adsorption/desorption equilibrium. The methyl orange solution periodically taken from the reactor was analyzed with a UV-visible spectrophotometer (PUXI TU-1810, Beijing, PR China). The analytical wavelength selected for the optical absorbance measurements was 464 nm.

RESULTS AND DISCUSSION

Photocatalytic activities: Fig. 1 illustrates the photocatalytic degradation of methyl orange using TiO_2 nanotubes and CdS-TNTAs. As for the pristine TiO_2 nanotube arrays, the degradation efficiency of methyl orange after 3 h test period is only 7.03 %, which is relatively low. The photocatalytic efficiencies for $CdS_{0.5min/20C}$-TNTAs, $CdS_{1min/10C}$-TNTAs, $CdS_{5min/2C}$-TNTAs and $CdS_{10min/1C}$-TNTAs are improved to 12.06, 12.56, 23.73 and 24.87 %, respectively, which demonstrates that CdS- sensitization can enhance the photodegradation efficiency. The kinetics of the degradation process can be evaluated by the following equation[7],

$$\ln \frac{C_0}{C} = \ln \frac{A_0}{A} = kt$$

where C_0 and C are the concentrations of methyl orange solution before and after degradation tests, A_0 is the absorbance of methyl orange solution at a wavelength of 464 nm measured before degradation tests, A is the absorbance after degradation for a period of time t and k is the degradation rate constant. The reaction kinetics is undergone by linear fit and the corresponding kinetic constants as using TiO_2 nanotubes, $CdS_{0.5min/20}$C-TNTAs, $CdS_{1min/10C}$-TNTAs, $CdS_{5min/2C}$-TNTAs and $CdS_{10min/1C}$-TNTAs are approximately 0.024, 0.043, 0.048, 0.090 and 0.095 h^{-1}, respectively, which are listed in Table-2. Clearly, the degradation using CdS-TNTAs as photocatalysts is much faster than that using the pristine TiO_2 nanotubes.

TABLE-2
KINETIC CONSTANTS k AND REGRESSION COEFFICIENTS (R) OF METHYL ORANGE DEGRADATION USING TIO_2 NANOTUBES AND CdS-TNTAs

Photocatalysts	k (h^{-1})	R^2
TiO_2 nanotubes	0.024	0.995
$CdS_{0.5min/20C}$-TNTAs	0.043	0.997
$CdS_{1min/10C}$-TNTAs	0.048	0.996
$CdS_{5min/2C}$-TNTAs	0.090	0.996
$CdS_{10min/1C}$-TNTAs	0.095	0.998

It is noted that besides the degradation using CdS-TNTAs as photocatalysts is much faster than that using the pristine TiO_2 nanotube arrays, the degradation rates and efficiencies using $CdS_{5min/2C}$-TNTAs and $CdS_{10min/1C}$-TNTAs as photocatalysts are much higher than those using $CdS_{0.5min/20}$C-TNTAs and $CdS_{1min/10C}$-TNTAs. To elucidate such phenomena, the characterization on the composition, morphology and UV-visible absorption of the samples were performed as follows.

Composition: The chemical composition of the CdS-TNTAs sample is investigated by XPS. The existence of elements Ti, O, Cd, S and also C is confirmed from the spectrum

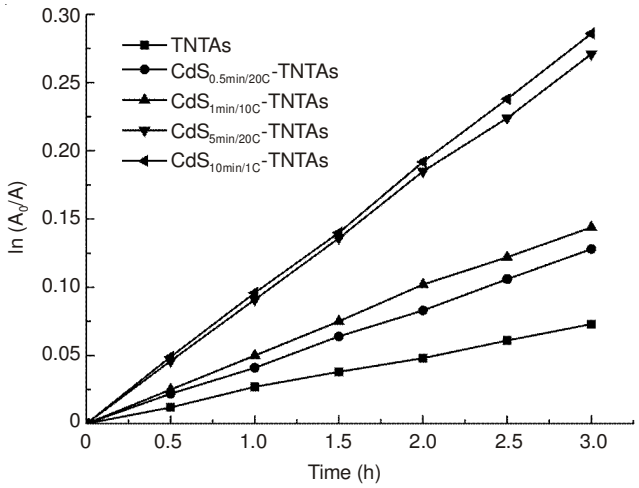

Fig.1. Photocatalytic degradation of methyl orange using TiO_2 nanotube arrays and CdS-TNTAs

of the sample. Fig. 2a and b show the high resolution XPS spectra of Cd3d and S2p, respectively. The Cd3d XPS spectrum (Fig. 2a) has two peaks at 405.6 eV ($3d_{5/2}$) and 412.3 eV ($3d_{3/2}$), in good agreement with the published values for CdS[25,27]. The S2p XPS spectrum shown in Fig. 2b indicates that the sulfur element exists as two chemically distinct species in the sample. The low and broad peak centered at 168.6 eV is assigned to sulfur in sulfate, for reaction with humid environments causes the sample surface of sulfide to oxidize and form sulfate[25,28]. The peak with a split that is near 1 e V and the area ration is 2:1,

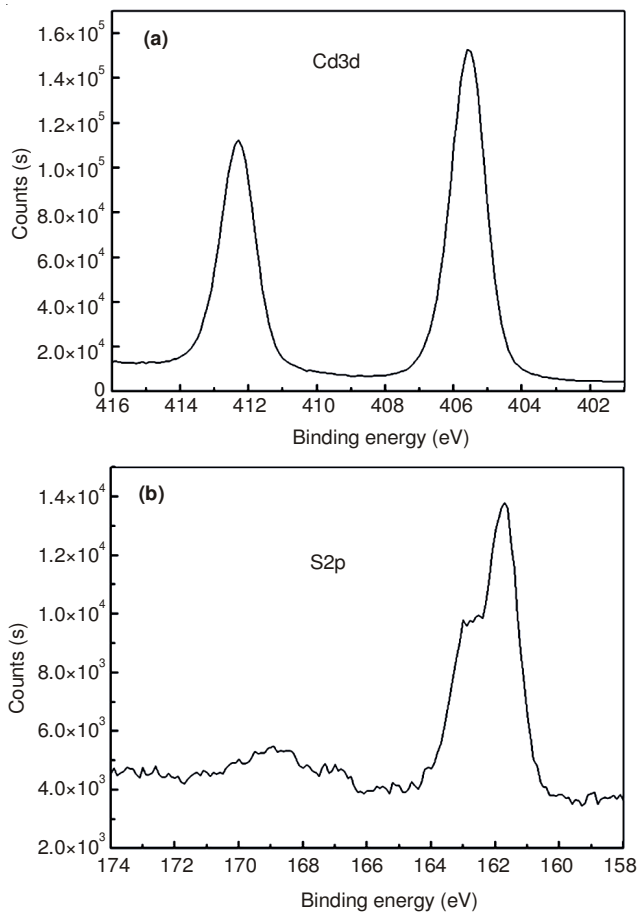

Fig. 2. XPS (a) Cd3d spectrum, (b) S2p spectrum of the CdS-TNTAs sample

is for sulfide, which occurs because of the split between $S2p_{3/2}$ (161.7 eV) and $S2p_{1/2}$ (162.7 eV), in consistent with the published values of the S2p signal for CdS[25,27]. Thus CdS is identified not only from the peaks at 405.6 eV of Cd $3d_{5/2}$ and 412.3 eV of Cd $3d_{3/2}$, but also from the peaks at 161.7 eV of $S2p_{3/2}$ and 162.7 eV of $S2p_{1/2}$.

Morphology: Fig. 3 shows the FE-SEM images of TiO_2 nanotubes (a, b), $CdS_{0.5min/20C}$-TNTAs (c, d) and $CdS_{5min/2C}$-TNTAs (e, f). The pristine TiO_2 nanotubes (Fig. 3a: top-view, Fig. 3b: cross-sectional view) have an average diameter of 95 nm and with a length of approximate 1.1 μm. The top surface view of $CdS_{0.5min/20C}$-TNTAs (Fig. 3c) illustrates that TiO_2 nanotubes have been extensively covered with a layer of CdS nanoparticles in diameter from 20 to 30 nm with some degree of aggregation, implying a high degree of CdS loading. Fig. 3d is the cross-sectional view of $CdS_{0.5min/20C}$-TNTAs, which indicates that some CdS nanoparticles reside within the TiO_2 nanaotubes. While for the $CdS_{5min/2C}$-TNTAs sample (Fig. 3e: top-view, Fig. 3f: cross-sectional view), the well-ordered nanotube structure is obvious and the CdS nanoparticles randomly distribute on TiO_2 nanotubes, indicating a low degree of CdS loading.

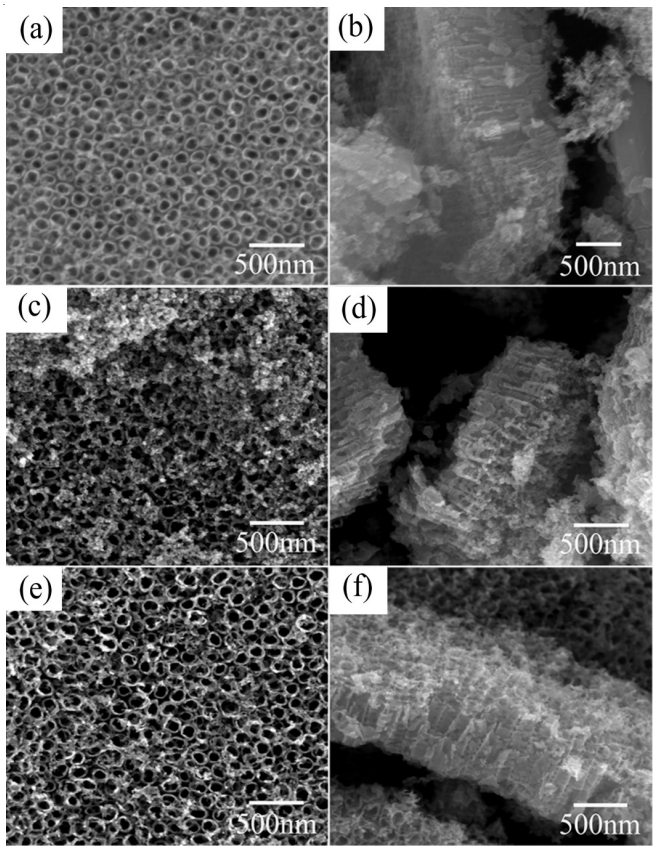

Fig. 3. FE-SEM micrographs of (a, b) TiO_2 nanotube arrays, (c, d) $CdS_{0.5min/20C}$-TNTAs and (e, f) $CdS_{5min/2C}$-TNTAs

UV-visible absorption: Fig. 4 shows the UV-visible absorption spectra of TiO_2 nanotubes, $CdS_{0.5min/20C}$-TNTAs and $CdS_{5min/2C}$-TNTAs. Clearly, TiO_2 nanotubes have a strong band edge absorption at 75 nm, which limits their use as a heterogeneous catalyst operating with excitation in the visible range. The deposition of CdS makes the band edge absorption red-

shifted to 400 nm for the $CdS_{0.5min/20C}$-TNTAs sample and to 515 nm for the $CdS_{5min/2C}$-TNTAs sample, which implies that CdS-TNTAs can be used under excitation in the violet-blue region of the electromagnetic spectrum. The red shift in the band edge absorption reflects the change of the band gap energy[29]. The calculated band gap energies are 3.30 eV for TiO_2 nanotubes, 3.10 eV for $CdS_{5min/2C}$-TNTAs and 2.40 eV for $CdS_{0.5min/20C}$-TNTAs. The $CdS_{0.5min/20C}$-TNTAs have a typical band gap energy value for bulk CdS[25], which suggests that deposition of CdS under the condition of immersion time 0.5 min and cycles 20 led to a very high degree of CdS loading just as that observed from FE-SEM images in Fig. 3c.

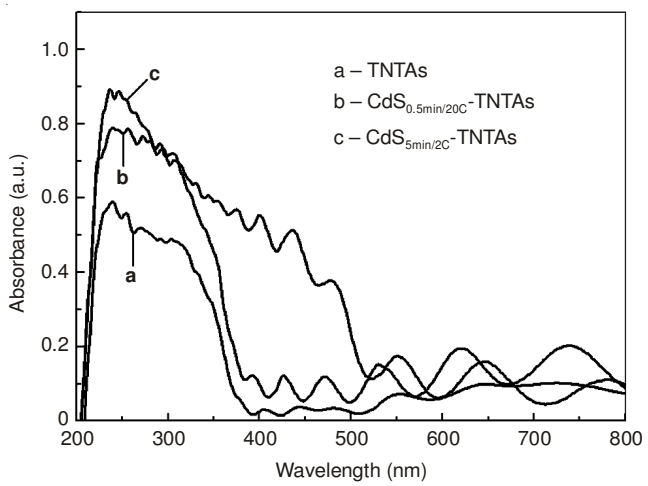

Fig. 4. Diffuse reflectance UV-visible spectra of the TiO_2 nanotubes, $CdS_{0.5min/20C}$-TNTAs, and $CdS_{5min/2C}$-TNTAs samples

In combination of all the above results, the achieved high photocatalytic efficiency of CdS-TNTAs can be well understood. TiO_2 is an *n*-type semiconductor with wide band gap, which only has absorption in UV light region. When the pristine TiO_2 nanotubes is activated under UV light, the excited electrons will immediately transfer from its valence band (VB) to conduction band (CB), leaving the holes in VB. However, the lifetime of the photogenerated electrons and holes is very short and they will recombine rapidly[1-4]. The band gap of CdS (2.4 eV) is lower than that of TiO_2, so when illuminated by light source, CdS is excited first and the electron/hole pairs are generated. Since the CB of CdS is more negative than that of TiO_2, excited electrons from CdS can quickly transfer to TiO_2 nanotubes, whereas holes can accumulated in CdS[20-26]. Thus, the interfacial electron transfer from CdS to TiO_2 nanotubes can effectively separate the electrons and holes, inhibiting the recombination of electron/hole pairs. Electrons will react with oxygen absorbed on the surface of TiO_2 nanotubes to form super-oxide radicals, $^{\bullet}O_2^-$. A positive charged hole will react with OH^- or H_2O to generate $^{\bullet}OH$. The super-oxide radical ion $^{\bullet}O_2^-$ and hydroxyl radical $^{\bullet}OH$ are responsible for the degradation of methyl orange. The above degradation process can be illustrated as follows[22,30,31]:

$$CdS + h\nu \rightarrow CdS\ (e^-) + CdS\ (h^+) \quad (1)$$

$$CdS\ (e^-) + TiO_2 \rightarrow CdS + TiO_2\ (e^-) \quad (2)$$

$$TiO_2\ (e^-) + O_2 \rightarrow TiO_2 + {}^{\bullet}O_2^- \quad (3)$$

$$CdS\ (h^+) + H_2O \rightarrow H^+ + {}^{\bullet}OH + CdS \quad (4)$$

$$CdS\ (h^+) + OH^- \rightarrow {}^{\bullet}OH + CdS \quad (5)$$

$$^{\bullet}O_2^-\ (^{\bullet}OH) + MO \rightarrow \text{degradated products} \quad (6)$$

Moreover, the effects of the immersion time and cycles of S-CBD treatment on the photocatalytic activities of CdS-TNTAs can be explained. The photocatalytic performance of CdS-TNTAs is speculated to result from a compromise between a larger amount of light absorption and a lower efficiency of charge separation, as well as limited diffusion by channel blocking at a higher degree of CdS loading[23]. As the whole S-CBD treatment duration keeps constant, the shorter immersion time in every solution and more cycles can cause higher degree of CdS loading. Hence, though $CdS_{0.5min/20C}$-TNTAs in the present work have very narrow band gap (2.40 eV) that facilitate light absorption, the high degree of CdS loading results in agglomeration of CdS nanoparticles (Fig. 3c) which decreases the charge separation efficiency and baffles the charge diffusion by blocking the channels. Thus, the photocatalytic performance of $CdS_{0.5min/20C}$-TNTAs is poorest as compared with those of $CdS_{1min/10C}$-TNTAs, $CdS_{5min/2C}$-TNTAs and $CdS_{10min/1C}$-TNTAs. Therefore, optimizing the deposition condition, such as the immersion time and cycles of S-CBD treatment, to achieve an ideal compromise between light absorption and charge separation/diffusion, is important for improving the photocatalytic ability of CdS-TNTAs. In the present work, $CdS_{5min/2C}$-TNTAs and $CdS_{10min/1C}$-TNTAs samples have much better photocatalytic performance, whose rate constants of degrading methyl orange are about 4 times higher than that using the pristine TiO_2 nanotubes.

Conclusion

CdS-TNTAs were prepared by depositing CdS into the crystallized anodic TiO_2 nanotubes *via* sequential chemical bath deposition (S-CBD) method. The CdS nanoparticles, approximately 20-30 nm in diameter, were deposited on TiO_2 nanotube arrays. CdS-sensitization extended the absorption response of TiO_2 nanotubes into the visible region. The photocatalytic efficiency of CdS-TNTAs was significantly enhanced as compared to the pristine TiO_2 nanotubes, which could be attributed to the deposition of CdS effectively stimulating charge separation and thus hindering the recombination of electron/hole pairs of TiO_2 nanotubes. Moreover, the immersion time and cycles of S-CBD treatment were found to have important impacts on the photocatalysis efficiencies of CdS-TNTAs. The appropriate immersion time and cycles of S-CBD process benefit the photocatalysis. $CdS_{5min/2C}$-TNTAs and $CdS_{10min/1C}$-TNTAs samples prepared in the present work exhibited much better photocatalytic performance, whose rate constants of degrading methyl orange are about 4 times higher than that using TiO_2 nanotubes. Taking the advantage of efficient charge separation, CdS-TNTAs fabricated in the present work can be used not only as the important photocatalysts in degradation of organic compounds but also as the promising photoelectrodes for photoelectrocatalysis or solar cell applications.

ACKNOWLEDGEMENTS

The authors acknowledged the financial support from the National Natural Science Foundation of China (21373281, 21273293), the Natural Science Foundation of CQ (CSTC-

2011AB4056), the Program for New Century Excellent Talents in University (NCET-12-0587), the Fundamental Research Funds for the Central Universities (CDJZR13225501) and the sharing fund of Chongqing University's Large-scale Equipment.

REFERENCES

1. P. Roy, S. Berger and P. Schmuki, *Angew. Chem. Int. Ed*., **50**, 2904 (2011).
2. S. Rani, S.C. Roy, M. Paulose, O.K. Varghese, G.K. Mor, S. Kim, S. Yoriya, T.J. LaTempa and C.A. Grimes, *Phys. Chem. Chem. Phys*., **12**, 2780 (2010).
3. Y.C. Nah, I. Paramasivam and P. Schmuki, *Chem. Phys. Chem*, **11**, 2698 (2010).
4. A. El Ruby Mohamed and S. Rohani, *Energy Environ. Sci*., **4**, 1065 (2011).
5. G.H. Liu, K.Y. Wang, N. Hoivik and H. Jakobsen, *Sol. Energy Mater. Sol. Cells*, **98**, 24 (2012).
6. J.M. Macak, M. Zlamal, J. Krysa and P. Schmuki, *Small*, **3**, 300 (2007).
7. G.G. Zhang, H.T. Huang, Y.S. Liu and L.M. Zhou, *Appl. Catal. B*, **90**, 262 (2009).
8. G.G. Zhang, H.T. Huang, Y.H. Zhang, H.L.W. Chan and L.M. Zhou, *Electrochem. Commun*., **9**, 2854 (2007).
9. M. Kalbacova, J.M. Macak, F. Schmidt-Stein, C.T. Mierke and P. Schmuki, *Phys. Status Solidi RRL*, **2**, 194 (2008).
10. X.W. Kang and S.W. Chen, *J. Mater. Sci*., **45**, 2696 (2010).
11. V. Jaeger, W. Wilson and V.R. Subramanian, *Appl. Catal. B*, **110**, 6 (2011).
12. L. Li, Z. Zhou, J. Lei, J. He, S. Zhang and F. Pan, *Appl. Surf. Sci*., **258**, 3647 (2012).
13. J.J. Liao, S.W. Lin, L. Zhang, N.Q. Pan, X.K. Cao and J.B. Li, *ACS Appl. Mater. Interfaces*, **4**, 171 (2012).
14. Y.F. Tu, S.Y. Huang, J.P. Sang and X.W. Zou, *J. Alloys Comp*., **482**, 382 (2009).
15. J. Xu, Y. Ao, M. Chen and D. Fu, *Appl. Surf. Sci*., **256**, 4397 (2010).
16. Y.L. Su, X.W. Zhang, M.H. Zhou, S. Han and L.C. Lei, *J. Photochem. Photobiol. A*, **194**, 152 (2008).
17. H.J. Liu, G.G. Liu and Q.X. Zhou, *J. Solid State Chem*., **182**, 3238 (2009).
18. S.Y. Kuang, L.X. Yang, S.L. Luo and Q.Y. Cai, *Appl. Surf. Sci*., **255**, 7385 (2009).
19. S.S. Zhang, S.Q. Zhang, F. Peng, H.M. Zhang, H.W. Liu and H.J. Zhao, *Electrochem. Commun*., **13**, 861 (2011).
20. J.C. Kim, J. Choi, Y.B. Lee, J.H. Hong, J.I. Lee, J.W. Yang, W.I. Lee and N.H. Hur, *Chem. Commun.*, **48**, 5024 (2006).
21. Q. Zhou, M.L. Fu, B.L. Yuan, H.J. Cui and J.W. Shi, *J. Nanopart. Res*., **13**, 6661 (2011).
22. D.W. Jiang, T.S. Zhou, Q. Sun, Y.Y. Yu, G.Y. Shi and L.T. Jin, *Chin. J. Chem*., **29**, 2505 (2011).
23. J.K. Ryu, S.H. Lee, D.H. Nam and C.B. Park, *Adv. Mater*., **23**, 1883 (2011).
24. W.T. Sun, Y. Yu, H.Y. Pan, X.F. Gao, Q. Chen and L.M. Peng, *J. Am. Chem. Soc*., **130**, 1124 (2008).
25. S.G. Chen, M. Paulose, C.M. Ruan, G.K. Mor, O.K. Varghese, D. Kouzoudis and C.A. Grimes, *J. Photochem. Photobiol. A*, **177**, 177 (2006).
26. S. Banerjee, S.K. Mohapatra, P.P. Das and M. Misra, *Chem. Mater*., **20**, 6784 (2008).
27. M. Kundu, A.A. Khosravi, S.K. Kulkarni and P. Singh, *J. Mater. Sci*., **32**, 245 (1997).
28. K. Bandyopadhyay, K.S. Mayya, K. Vijayamohanan and M. Sastry, *J. Electr. Spectrosc*., **87**, 101 (1997).
29. B.C. Viana, O.P. Ferreira, A.G. Souza Filho, C.M. Rodrigues, S.G. Moraes, J. Mendes Filho and O.L. Alves, *J. Phys. Chem. C*, **113**, 20234 (2009).
30. X.Q. Li, L.F. Liu, S.Z. Kang, J. Mu and G.D. Li, *Catal. Commun*., **17**, 136 (2012).
31. G.S. Li, D.Q. Zhang and J.C. Yu, *Environ. Sci. Technol*., **43**, 7079 (2009).